Journal of Materials Chemistry A

Accepted Manuscript

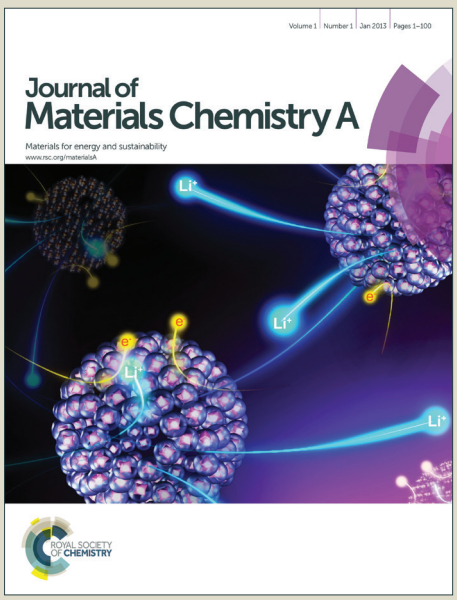

This is an *Accepted Manuscript*, which has been through the Royal Society of Chemistry peer review process and has been accepted for publication.

Accepted Manuscripts are published online shortly after acceptance, before technical editing, formatting and proof reading. Using this free service, authors can make their results available to the community, in citable form, before we publish the edited article. We will replace this *Accepted Manuscript* with the edited and formatted *Advance Article* as soon as it is available.

You can find more information about *Accepted Manuscripts* in the Information for Authors.

Please note that technical editing may introduce minor changes to the text and/or graphics, which may alter content. The journal's standard Terms & Conditions and the Ethical guidelines still apply. In no event shall the Royal Society of Chemistry be held responsible for any errors or omissions in this *Accepted Manuscript* or any consequences arising from the use of any information it contains.

ROYAL SOCIETY OF CHEMISTRY

www.rsc.org/materialsA

Journal Name
Journal of Materials Chemistry A
Dynamic Article Links ►

Cite this: DOI: 10.1039/c0xx00000x

www.rsc.org/xxxxxx

ARTICLE TYPE

Spiro-thiophene Derivative as Hole-transport Materials for Perovskite Solar Cells

Shuying Ma,[a] Hua Zhang,[a] Ning Zhao,[a] Yibing Cheng,[b] Mingkui Wang,*[a] Yan Shen and Guoli Tu*[a]

Received (in XXX, XXX) Xth XXXXXXXXX 20XX, Accepted Xth XXXXXXXXX 20XX
DOI: 10.1039/b000000x

This work reports on a promising hole transporting material using of spiro-thiophene derivative with 4,4'-spirobi [cyclopenta[2,1-b;3,4-b']dithiophene] as the spiro core for perovskite solar cells, exhibiting an overall power conversion efficiency of 10.4% with an open circuit voltage of 0.94 V, a short circuit current density of 16.54 mA cm^{-2} under standard testing condition.

Introduction

Perovskite solar cells are drawing great attentions due to their advantages of low cost and high efficiency. This solution processable solar cell is promising for large scale thin film photovoltaic technology application. The power conversion efficiency (PCE) of this type solar cell has been rapidly increased from 3.8% to 20.1% during the past few years due to the application of all-solid-state thin-film architecture and interfacial engineering.[1-7] In most of highly efficient perovskite solar cell devices, organic hole conductor are commonly used for hole transport purposes.[8,9] To date, the amorphous organic (2,2-7.7-tetrakis(N,N'-diparamethoxy-phenyl-amine 9,9'-spirobifluorene) (spiro-OMeTAD) is the most popular hole transport material (HTM) for pervoskite solar cells, which has been extensively studied due to its good solubility, weak absorption within the scope of visible light, good film-forming property, and high hole mobility.[10-13] spiro-OMeTAD was firstly introduced into solid-state sensitized mesoporous heterojunction solar cells.[14] Though the charge transfer from the sensitizers to spiro-OMeTAD in the heterojunction is very efficient, the overall PCE of the devices is relatively low due to a fast charge recombination at the dye-sensitized TiO_2/spiro-OMeTAD interface as discovered latterly.[15] Since the first report on the lead iodide perovskite sensitized all-solid-state thin film mesoscopic solar cell using spiro-OMeTAD as hole conductor, the PCE of this type of solar cell has already exceeded 15% by finely tuning interfacial energy levels and controlling thin film morphologies.[16] The spiro-OMeTAD as an expensive organic hole conducting organic material has to face with disadvantages of poor crystallinity, and possible degradation under environmental influences. Furthermore, a strong accumulation of charge has been found to take place in the pervoskite layer upon exposure to light by mapping the contact potential difference between tip and sample within Kelvin probe force microscopy measurement.[17,18] A comparison of the electrical potential distribution before and after illumination of the device revealed a persistent positive charging in the mesoporous TiO_2 layer and negative charging inside the pervoskite capping layer.[17] The positive charging, which could be due to the TiO_2 electron conductor works much effectively than spiro-OMeTAD, may change the electric field in the hetrojunction and slow down the charge transport. Therefore, several alternatives have been proposed to spiro-OMeTAD, aiming for enhancement of hole conductivity and durability.[17,18] For example, the use of a polymeric hole conductor, especially poly-triarylamine, substantially improves the open-circuit voltage V_{oc} and fill factor of the cells, yielding a power conversion efficiency of 12.0% under standard AM 1.5 conditions.[19] Recently, various organic HTMs have been reported in efficient pervoskite solar cells, such as tetrathiafulvalene derivatives[20], pyrene-core arylamine derivatives[21], quinolizino acridine compounds[22], 3,4-ethylenedioxythiophene[23], carbazole derivatives[24], and polyfluorene derivatives[25], showing PCEs in the range of 11-14%. These hole conductors have great potential to replace the expensive spiro-OMeTAD because of their much simpler and cheaper synthesis, which promote the advancement of cost-effective and practical perovskite solar cells.

The concept of spiro is used to improve the morphological stability of low molar mass materials and retain their electronic properties as well by connecting two more or less extended π-systems via a common sp^3-hybridized atom.[26] As a promising class of material for organic optoelectronics, the spiro compounds offer several benefits. For instance, the perpendicular arrangement of the two moieties leads to rigid structure, efficiently suppressing molecular interactions between the π-systems which can reduce tendency to form aggregates. Hence, the introduction of the spiro structure raises the resulted compounds' glass temperature (T_g) and improves morphological stability in the solid state. For example, the glass transition temperature of spiro-OMeTPA is reported to be 125 ^oC, being higher than that of the counterpart compound *N*,*N'*-diphenyl-*N*,*N'*-bis(3-methylphenyl) 4,4'- diamine (TPD) (T_g = 62 ^oC).[26,27] Crystallization of the hole conductor layer is undesirable for it would impair the formation of a good contact among the active layer and back contact electrodes. Furthermore, the spiro compound has been found to be highly solvable in commonly used solvents compared to the corresponding non-spiro-linked parent compounds.[28,29] Spiro-type compounds based on the 9,9'-spirobifluorene core have been intensively studied in the recent years. Several compounds based on this core have been

Journal of Materials Chemistry A Accepted Manuscript

successfully synthesized and applied in organic solar cells, organic light-emitting devices, field-effect transistors and lasers.[30-33] In order to expand the spiro family, the thiophene-based spiro core, 4,4'-spirobi[cyclopenta[2,1-b;3,4-b']dithiophene] (SCPDT), has been developed by Salbeck and co-workers as a new heterocyclic building block.[34] It has been observed that the optical, electrochemical and electrical properties of the derivatives using SCPDT spiro core are very different to those analogues with 9,9'-spirobifluorene. In comparison with the 9,9'-spirobifluorene using benzene as the block unit, the SCPDT is ready for redox reaction due to the thiophene having higher electron density and lower aromaticity properties. Therefore, the SCPDT derivatives are very promising as charge transport materials in organic electronics devices.[35-37] In this work, 5-octyl-2,2'-bithiophene units are combined with the sprio core of SCPDT to form a new compound, which is used as hole conductor for pervoskite solar cell application.

Experimental section

Material synthesis

The synthesis details and characterization of the SCPDT-BiT is described in the supporting information (Figures S1-2).

Device fabrication

For hole mobility testing, a conventional structure of ITO/PEDOT:PSS(40 nm)/SCPDT-BiT/MoO_3/Au (60 nm) was fabricated. SCPDT-BiT (20 mg) was dissolved in 1 mL 1,2-dichlorobenzene (DCB) and stirred overnight. The pre-cleaned ITO substrate was treated with UV-ozone for 25 min, and then a 40 nm PEDOT:PSS layer was spin-coated on the ITO substrate from an aqueous solution (Baytron P VP AI 4083), followed by baking in an oven at 150 °C for 10 min. The active layer was obtained by spin-coating the SCPDT-BiT solution at 600 rpm for 2 min in a glove box. The active layer thickness (~142 nm) was measured with a Dektek profilometer. A bilayer cathode structure of MoO_3(10 nm)/Au (60 nm) was thermally evaporated atop the active layer in vacuum chamber under a base pressure of about 2×10^{-4} Pa. The device active area was 0.16 cm^2, which was defined by the overlapping area of the ITO and Au electrodes. For comparison, the devices with spiro-MeOTAD were fabricated with the same condition.

Solar cell device Preparation: Fluorine-doped tin oxide (F:SnO_2) coated glass (Pilkington TEC 15, 15 Ω/square) was patterned by etching with Zn powder and 2 M HCl diluted in milliQ water. The etched substrate was then cleaned with 2% hellmanex diluted in milliQ water, rinsed with milliQ water, and ethanol and dried with clean dry air. The substrate was underwent in a UV-O_3 chamber for 30 min prior to spray pyrolysis at 500 ^oC using 40 mL of a titanium diisopropoxidebis (acetylacetonate) solution (75% in 2-propanol, Sigma-Aldrich) diluted in ethanol (1:39, v/v) and oxygen as carrier gas, and sintered on a hot plate for 1 h at 500 ^oC. The TiO_2 compact layer thickness was ~30 nm. Porous TiO_2 films of 200 nm thick were deposited onto compact layer covered substrates by spin coating at 5000 rpm for 30 s using a TiO_2 paste (Dyesol 30 NRD, 30 nm average particle size) diluted in anhydrous ethanol (1:3, weight ratio). After drying at 120 ^oC, the TiO_2 layers were heated to 500 ^oC for 30 min. The mesoporous TiO_2 films were infiltrated with PbI_2 by spin-coating a PbI_2 solution in DMF (508 mg mL^{-1}) that was kept at 70 ^oC. After drying, the films were dipped in a solution of CH_3NH_3I in 2-propanol (10 mg mL^{-1}) for 30 s and rinsed with 2-propanol and dried at 70 ^oC for 30 min. After drying, the $CH_3NH_3PbI_3$-adsorbed films were covered with HTM layer by spin coating at 4000 rpm for 30 s in the glove box. The HTM recipe was prepared by dissolving 78.3 mg of 2-(5'-hexyl-2',3'-dihydro-[2,2'-bithiophen]-5-yl)-2',6,6'- tris(5'-hexyl-[2,2'-bithiophen]-5-yl)-4,4'-spirobi[cyclopenta[1,2-b:5,4-b']dithiophene], 28.8 μL of 4-tert-butyl-pyridine, and 17.5 μL of a stock solution of 520 mg mL^{-1} lithium bis-(trifluoromethylsulfonyl)imide in acetonitrile in 1 mL of chlorobenzene. Finally, 65 nm of gold was thermally evaporated in the vacuum chamber on top of the device to form the electrode contacts. The device fabrication was carried out under controlled atmospheric conditions and a humidity of <1.0 ppm.

The solar cell device was fabricated with spiro-OMeTAD for comparison. The HTM recipe was prepared by dissolving 72.3 mg of Spiro-OMeTAD, 28.8 μL of 4-tert-butylpyridine, and 17.5 μL of a stock solution of lithium salt in 1 mL of chlorobenzene.

Device characterization

A solar simulator with a Xe light source (450 W, Oriel, model 9119) and an AM 1.5G filter (Oriel, model 91192) was used to give an irradiance of 100 mW cm^{-2} at the surface of the solar cell. The current-voltage characteristics of the cell under these conditions were obtained by applying an external potential bias to the cell and measuring the generated photocurrent on a Keithley model 2400 digital source meter (USA). A similar data-acquisition system was used to control the IPCE measurements. A white-light bias (10 % sunlight intensity) was applied onto the sample during the IPCE measurements with the AC model (10 Hz).

The photovoltage/photocurrent transient decay measurement was carried out to obtain the electronic diffusion length (HuaMing, model 201501). A white light bias on the device sample was generated from an array of diodes. Blue light pulse diodes (0.05 s square pulse width, 100 ns rise and fall time) controlled by a fast solid-state switch were used as the perturbation source. The voltage dynamics were recorded on a PC-interfaced Keithley 2602A source meter with a 100 μs response time. The perturbation light source was set to a suitably low level in order for the voltage decay kinetics to be monoexponential. By varying the white light bias intensity, the diffusion length could be estimated over a range of applied biases.

Results and discussion

In this study, we report on a new material based on the SCPDT core as HTM for PSCs application for the first time. The 4,4'-spirobi[cyclopenta[2,1-b;3,4-b']dithiophene] with four 5-octyl-2,2'-bithiophene as rigid arms (coded as SCPDT-BiT) can be obtained by a standard Pd-mediated Stille coupling reaction with yield of 54% (Scheme 1). The molecular structure of SCPDT-BiT is presented in Scheme 1. The resultant SCPDT-BiT exhibits excellent solubility in organic solvents such as chloroform and toluene. The structure and purity of all the intermediates and final compounds were identified by NMR and high-resolution mass spectrometry (see Figures S1 and S2 in supporting information). Figure 1a compares the UV-visible absorption spectroscopy of SCPDT-BiT and spiro-OMeTAD. In toluene solution, the

Journal of Materials Chemistry A Accepted Manuscript

This journal is © The Royal Society of Chemistry [year]

SCPDT-BiT shows two absorption bands around 322 nm and 467 nm while spiro-OMeTAD shows two absorption bands at 306 nm and 388 nm. Table 1 lists the optoelectronic prosperities of the SCPDT-BiT and spiro-OMeTAD samples. Compared with the absorption of spiro-OMeTAD taking place in the UV-visible region, the SCPDT-BiT absorbs part of the visible light. It can be ascribed to the electron donating property of the bithiophene group. When directly bonding to the SCPDT core, the 5-octyl-2,2'-bithiophene units can largely increase the electron density of the SCPDT core. Thus, the SCPDT-BiT has a lager conjugated structure compared to spiro-OMeTAD. For the thin film of SCPDT-BiT, the absorption maximum peak is blue shifted to 457 nm with a shoulder peak at 525 nm. Both SCPDT-BiT and spiro-OMeTAD samples in the liquid solvents show the similar absorption with those of solid states, indicating a poor π-π intermolecular interaction in their thin-film states. This can be further proved by the XRD characterization. The appearance of strong peak at $2\theta = 18.9^{\circ}$ is ascribed to the Si substrate (Figure 2a). In the XRD pattern, no obvious peak representing the crystallization of SCPDT-BiT is observed.

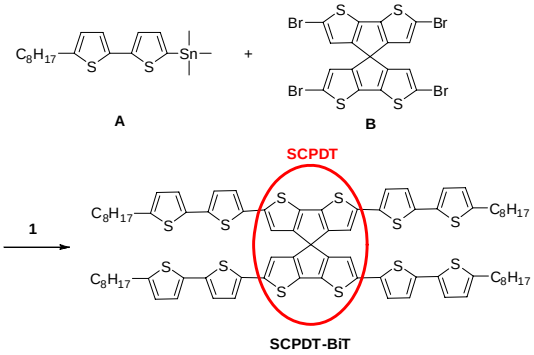

Scheme 1. Synthesis of SCPDT-BiT. 1: $Pd(PPh_3)_4$, toluene, 110 °C, 48 h.

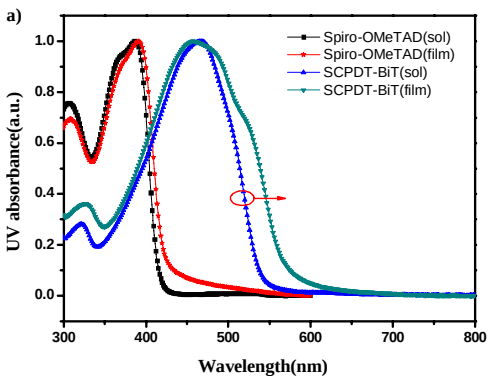

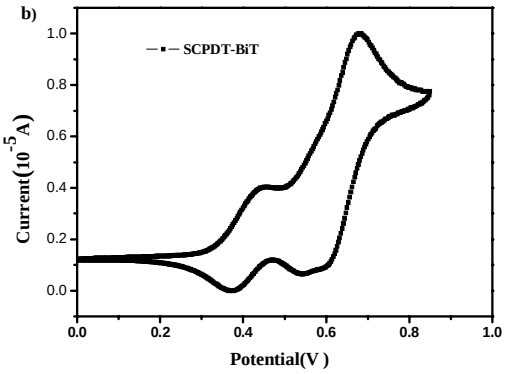

Fig. 1 a) Normalized absorption spectra of Spiro-OMeTPA and SCPDT-BiT in toluene and the thin-film state. b) CV spectra of SCPDT-BiT.

Table 1. Optical and electrochemical prosperities of the SCPDT-BiT and spiro-OMeTAD samples.

	λ_{max}[a] (nm)	λ_{max}[b] (nm)	$\Delta E_{gap\ (sol)}$[c] (eV)	HOMO[e] (eV)	LUMO[e] (eV)
SCPDT-BiT	467	457,525	2.25	-5.07	-2.82
Spiro-OMeTAD	387	391	2.95	-5.04	-2.09

[a] From UV-visible spectroscopy measurements on the samples in solution; [b] From UV-visible spectroscopy measurements the samples within solid-films [c] From absorption onset wavelength of the materials in solution. [d] From CV measurements;. [e] $E_{LUMO} = E_{HOMO} + \Delta E_{gap\ (sol)}$.

Cyclic voltammetry measurement was performed to investigate the electrochemical properties of SCPDT-BiT within anhydrous dichloromethane containing 0.1 M tetra-n-butylammonium hexafluorophosphate as a supporting electrolyte in a three electrode system. Figure 1b shows that the SCPDT-BiT undergoes two reversible one-electron oxidation processes with-half potentials at +0.37 V and +0.75 V vs. Fc/Fc^+.[34] Therefore, the HOMO energy level can be calculated on the basis of the following equation: $E_{HOMO} = -4.8 - \left(E_{ox} - E^{1/2}\left(Fc/Fc^{+}\right)\right)$, where E_{ox} is the onset oxidation potential (*vs.* Fc/Fc^+). The values of the E_{ox} for SCPDT-BiT and the $E^{1/2}$ for Fc/Fc^+ are 0.1 and 0.37 V (*vs.* Ag/AgCl). Therefore, the highest occupied molecular orbital (HOMO) level of SCPDT-BiT is estimated to be -5.07 eV, being slightly1c lower than that of spiro-OMeTAD (-5.04 eV, Table 1).[38,39] The extension of the conjugation length of SCPDT-BiT brings the HOMO energy level down compared with the SCPDT.[34] The HOMO level of SCPDT-BiT matches well with the valence-band level of the $CH_3NH_3PbI_3$ (~-5.44 eV), ensuring efficient driving force for hole transport from perovskite into HTM layer. The absorption onset wavelength for the SCPDT-BiT film is 550 nm, corresponding to optical energy gap of 2.25 eV. The LUMO energy level is thus calculated to be -2.82 eV.

Journal of Materials Chemistry A Accepted Manuscript

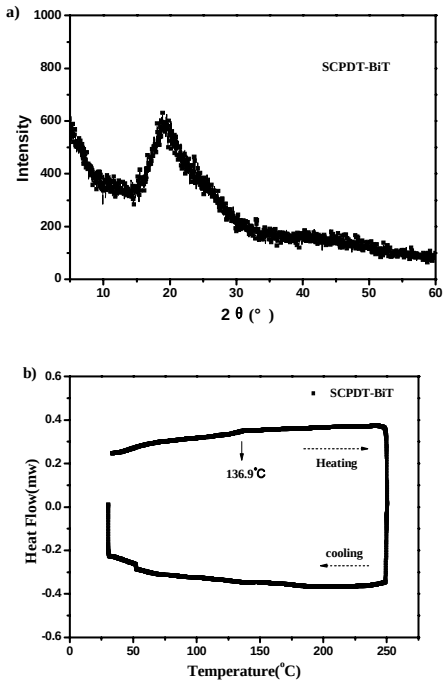

Fig. 2 a) XRD data of SCPDT-BiT film. b) Differential scanning calorimetry of SCPDT-BiT with glass transition at 136.9 °C.

Figure 2b presents the result of differential scanning calorimetry (DSC) measurement on the SCPDT-BiT. There is no obvious melting point observed from room temperature to 250 °C, suggesting that the SCPDT-BiT is an amorphous structure. The glass transition temperatures is evaluated to be 136.9 °C, which is higher than that of spiro-OMeTAD (T_g=125 °C) (Figure 2b). This result suggests that SCPDT-BiT can exhibit good thermal stability. A conventional structure of ITO/PEDOT:PSS (40 nm)/ SCPDT-BiT/MoO_3 (10 nm)/Au (60 nm) was fabricated for the measurement of hole mobility of SCPDT-BiT. The SCPDT-BiT without thermal annealing shows a hole mobility of 4.5×10^{-6} cm^2 V^{-1} s^{-1}. This can be improved by an order of magnitude after pre-anneal treatment at 100 °C for 10 min (5.96×10^{-5} cm^2 V^{-1} s^{-1}). The spiro-OMeTAD shows a hole mobility of 1.45×10^{-5} cm^2 V^{-1} s^{-1} in a same device structure without thermal annealing. After treatment at 100 °C for 10 min, the hole mobility of spiro-OMeTAD increases to 5.37×10^{-5} cm^2 V^{-1} s^{-1}. The high hole mobility for SCPDT-BiT could be attributed to the high charge-carrier mobility of thiophene unit.

Perovskite solar cells device were fabricated with the structure of FTO/TiO_2 (30 nm)/$CH_3NH_3PbI_3$ (300 nm)/SCPDT-BiT (120 nm)/Au (60 nm) with SCPDT-BiT as the hole transporting layer. Figure 3a presents the photocurrent-voltage curves of devices tested under 100 mW cm^{-2} AM 1.5G simulated irradiation. The open circuit voltage (V_{OC}), fill factor (FF), current density (J_{SC}) and power conversion efficiency of the device using SCPDT-BiT is 0.94 V, 0.67, 16.54 mA/cm^2 and 10.39% respectively. The reference device with spiro-OMeTAD as the hole conducting layer showsa V_{OC} of 0.95V, a FF of 0.67, a J_{SC} of 20.83 mA cm^{-2} with a PCE of 13.3%. The V_{OC} of SCPDT-BiT device is the slightly lower than that of spiro-OMeTAD. The device using SCPDT-BiT shows lower IPCE response in the range from 500 to 800 nm than that of device with spiro-OMeTAD (Figure 3b). This could be caused by fast interfacial charge recombination between pervoskite layer and the SCPDT-BiT layer.

Transient photovoltage/photocurrent decay measurements were performed to extract the photo-generated electron diffusion length for devices with different HTMs. The charge carrier diffusion length L was estimated by the equation of $L=\sqrt{D\cdot\tau}$, where D is the charge diffusion constant, and τ charge carrier lifetime. Figure 4 displays the calculated charge diffusion length as a function of light irradiation intensity. The diffusion length is estimated to be about 320 nm for the spiro-OMeTAD device, however, the SCPDT-BiT device shows a slightly shorter diffusion length (~300 nm). The charge collection can be determined by $\eta_{coll}=1/\left(1+(d/L_d)^2\right)$, where d^2 is the mean square displacement necessary for an electron to reach the $MAPbI_3/TiO_2$ interface from the point where it is photo-generated, and L_d is the diffusion length. Therefore, a 15% enhancement in the charge collection can be evaluated for the device using spiro-OMeTAD compared to that of device with SCPDT-BiT, which may explain a higher photocurrent in the former.[40]

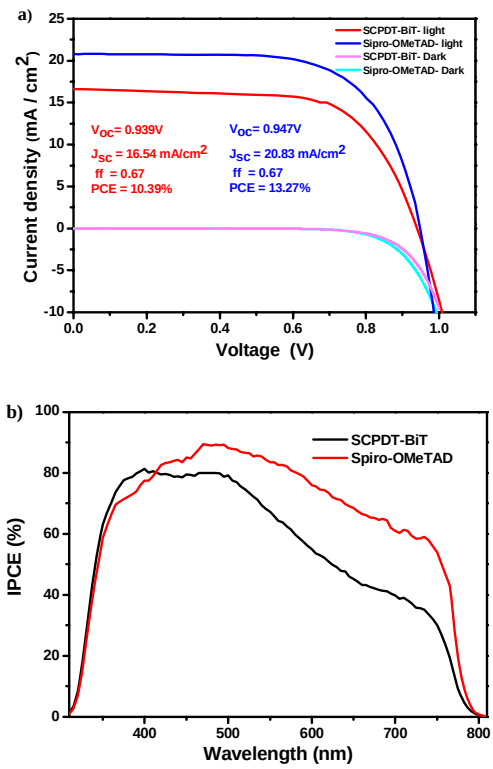

Fig. 3 J–V curves (a) and IPCE spectra (b) of the perovskite solar cells based on SCPDT-BiT and Spiro-OMeTAD.

Journal of Materials Chemistry A Accepted Manuscript

This journal is © The Royal Society of Chemistry [year]

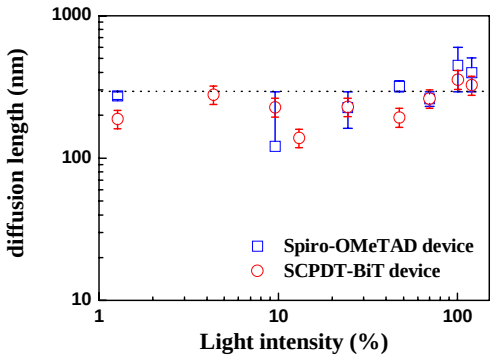

Fig. 4 The electron diffusion length (L, $L = \sqrt{D\tau}$) as a function of light intensity (% full sun intensity) obtained by transient photovoltage/photocurrent decay measurements.

Conclusions

In summary, a new spiro-thiophene derivative 2,2',6,6'-tetrakis(5'-octyl-[2,2'-bithiophen]-5-yl)-4,4'-spirobi[cyclopenta [1,2-b:5,4-b'] dithiophene] (SCPDT-BiT) has been synthesized and investigated as hole conducting layer for perovskite solar cells. The new HTM shows good PCE of over 10%. The results show that the spiro-thiophene derivatives are very promising candidates as hole transport material. Further efforts to increase the photocurrent by modifying the chemical structures and fine-tuning the device parameters are in progress.

Acknowledgement

The Financial support from the Director Fund of the WNLO, the 973 Program of China (2014CB643506 and 2013CB922104), and the NSFC (21161160445, 51073063 and 21274048), and the Fundamental Research Funds for the Central Universities (HUST: CXY12Q022) is acknowledged. The authors thank the Analytical and Testing Centre of Huazhong University of Science & Technology and the Center of Micro-Fabrication and Characterization (CMFC) of WNLO for the measurements of the samples.

Notes and references

[a] *Wuhan National Laboratory for Optoelectronics, Huazhong University of Science and Technology, Wuhan 430074, P. R. China. E-mail:* tgl@mail.hust.edu.cn, mingkui.wang@mail.hust.edu.cn

[b] *Department of Materials Engineering, Monash University, Melbourne, Australia*

† Electronic Supplementary Information (ESI) available: [the new hole transport material synthesis and characterzation]. See DOI: 10.1039/b000000x/

[1] P. Docampo, J. Ball, M. Darwich, G. Eperon and H. Snaith, Nat. commun., 2013, 4, 2761.
[2] J. Burschka, N. Pellet, S. -J. Moon, R. Humphry-Baker, P. Gao, M. K. Nazeeruddin and M. Grätzel, *Nature*, 2013, **499**, 316.
[3] G. Hodes, *Science*, 2013, **342**, 317.
[4] P. Boix, K. Nonomura, N. Mathews, S. Mhaisalkar, *Materials Today*, 2014, **17**, 16.[4]
[5] P. Qin, S. Tanaka, S. Ito, N. Tetreault, K. Manabe, H. Nishino, M. Nazeeruddin and M. Grätzel, *Nat. commun.*, 2014, **5**, 3834
[6] J. Cui, F. Meng, H. Zhang, K. Cao, H. Yuan, Y. Cheng, F. Huang and M. Wang, ACS *Appl. Mater. Interfaces*, 2014, **6**, 22862.
[7] http://www.nrea.org/content/nrea-member-services.
[8] D. Bi, G. Boschloo and A. Hagfeldt, *Nano*, 2014, **9**, 1440001.
[9] L. Polander, P. Pahner, M. Schwarze, M. Saalfrank, C. Koerner and K. Leo, *APL Mater.*, 2014, **2**, 081503.
[10] M. Wang, J. Liu, N. Cevey-Hua, S. Moon, P. Liska, r. Humphry-Baker, J. Moser, C. Grätzel, P. Wang, S. Zakeeruddin, M. Grätzel, *Nano Today*, 2010, **5**, 169.
[11] M. Wang, S. Moon, D. Zhou, N. Cevey-Hua, R. Humphry-Baker, C. Grätzel, P. Wang, S. Zakeeruddin, M. Grätzel, *Adv. Funct. Mater.*, 2010, **20**, 1821.
[12] J. Melas-Kyriazi, I. Ding, A. Marchioro, A. Punzi, B. Hardin, G. Burkhard, N. Tétreault, M. Grätzel, J. Moser and M. McGehee, *Adv. Energy Mater.*, 2011, **1**, 407.
[13] A. Dualeh, T. Moehl, M. Nazeeruddin and M. Grätzel, *ACS Nano.*, 2013, **7**, 2292.
[14] U. Bach, D. Lupo, P. Comte, J. E. Moser, F. Weissortel, J. Salbeck, H. Spreitzer and M. Grätze, *Nature*, 1998, **395**, 583.
[15] M. Wang, J. Bai, F. formal, S. Moon, L. Cevey-Ha, R. Humphry-Baker, C. Grätzel, S. Zakeeruddin and M. Grätzel, *J. Phys. Chem. C*, 2012, **116**, 3266.
[16] M. Liu, M. B. Johnston and H. J. Snaith, *Nature*, 2013, **501**, 395.
[17] V. Bergmann, S. Weber, F. Ramos, M. Nazeeruddin, M. Grätzel, D. Li, A. Domanski, I. Lieberwirth, S. Ahmad and R. Berger, *Nat. Commun.*, 2014, **5**, 5001.
[18] X. Xu, H. Zhang, K. Cao, J. Cui, J. Lu, X. Zeng, Y. Shen and M. Wang, *ChemSusChem*, 2014, **7**, 3088.
[19] J. Heo, S. Im, J. Noh, T. Mandal, C. Lim, J. Chang, Y. Lee, H. Kim, A. Sarkar, K. Nazeeruddin, M. Gratzel and S. Seok, *Nat. Photonics.*, 2013, **7**, 486.
[20] J. Liu, Y. Wu, C. Qin, X. Yang, T. Yasuda, A. Islam, K. Zhang, W. Peng, W. Chen and L. Han, *Energ. Environ. Sci.*, 2014, **7**, 2963.
[21] N. Jeon, J. Lee, J. Noh, M. Nazeeruddin, M. Gratzel and S. Seok, *J. Am. Chem. Soc.*, 2013, **135**, 19087.
[22] P. Qin, S. Paek, M. I. Dar, N. Pellet, J. Ko, M. Grätzel and M. Nazeeruddin, *J. Am. Chem. Soc.*, 2014, **136**, 8516.
[23] H. Li, K. Fu, A. Hagfeldt, M. Gratzel, S. Mhaisalkar and A. Grimsdale, *Angew. Chem., Int. Ed.*, 2014, **53**, 4085.
[24] S. Sung, M. Kang, I. T. Choi, H. Kim, H. Kim, M. Hong, H. Kim and W. Lee, *Chem. Commun.*, 2014, **50**, 14161.
[25] Z. Zhu, Y. Bai, H. Lee, C. Mu, T. Zhang, L. Zhang, J. Wang, H. Yan, S. So and S. Yang, *Adv. Fun. Mater.*, 2014, **24**, 7357.
[26] T. Saragi, T. Spehr, A. Siebert, T. Fuhrmann-Lieker and J. Salbeck, *Chem. Rev.*, 2007, **107**, 1011.
[27] T. Leijtens, I. Ding, T. Giovenzana, J. Bloking, M. McGehee, A. Sellinger, *ACS Nano*, 2012, **6**, 1455.
[28] T. Saragi, J. Londenberg and J. Salbeck, *J. Appl. Phys.*, 2007, **102**, 046104.
[29] G. Pozzi, S. Orlandi, M. Cavazzini, D. Minudri, L. Macor, L. Otero and F. Fungo, *Org. Lett.*, 2013, **15**, 4642.
[30] T. Spehr, R. Pudzich, T. Fuhrmann and J. Salbeck, *Org. Electron.*, 2003, **4**, 61.
[31] D. Schneider, T. Rabe, T. Riedl, T. Dobbertin, M. Kröger, E. Becker, H. Johannes, W. Kowalsky, T. Weimann, J. Wang, P. Hinze, A. Gerhard, P. Stössel, H. Vestweber, *Adv. Mater.*, 2005, **17**, 31.
[32] T. Spehr, A. Siebert, T. Fuhrmann-Lieker, J. Salbeck, T. Rabe, T. Riedl, H. Johannes, W. Kowalsky, J. Wang, T. Weimann and P. Hinze, *Appl. Phys. Lett.*, 2005, **87**, 161103.
[33] S. Ma, Y. Fu, D. Ni, J. Mao, Z. Xie and G. Tu, *Chem. Commun.*, 2012, **48**, 11847.
[34] J. Londenberg, T. Saragi, I. Suske and J. Salbeck, *Adv. Mater.*, 2007, **19**, 4049.
[35] S. Yang, Y. Kan, G. Yang, Z. Su and L. Zhao, *Chem. Phys. Lett.*, 2006, **429**, 180-184.
[36] S. Bouzzine, A. Makayssi, M. Hamidi, M. Bouachrine, *J. Mol. Struc-theochem*, 2008, **851**, 254.
[37] G. Pozzi, S. Orlandi, M. Cavazzini, D. Minudri, L. Macor, L. Otero, and F. Fungo, *Org. Lett.*, 2013, **15**, 4642.

Journal of Materials Chemistry A Accepted Manuscript

[38] K. Krishnamoorthy, F. Kunwu, P. Boix, H. Li, T. M. Kol, W. Leng, S. Power, A. Grimadal, M. Grätzel, N. Mathews and S. Mhaisalkar，*J. Mater. Chem. A.,* 2014, **2**, 6350.
[39] W. Nguyen, C. Bailie, E. Unger and M. McGehee, *J. Am. Chem. Soc.,* 2014, **136**, 10996.
[40] X. Xu, S. Li, H. Zhang, Y. Shen, S. Zakeeruddin, M. Graetzel, Y. Cheng and M. Wang, *ACS Nano*, 2015, **9**, 1782.

Journal of Materials Chemistry A Accepted Manuscript

This journal is © The Royal Society of Chemistry [year]

TOC

Spiro-thiophene Derivative as Hole-transport Materials for Perovskite Solar Cells

Shuying Ma, Hua Zhang, Ning Zhao, Yibing Cheng, Mingkui Wang and Guoli Tu

Spiro-thiophene derivative acts as promising hole transport material for highly efficient pervoskite solar cells application.

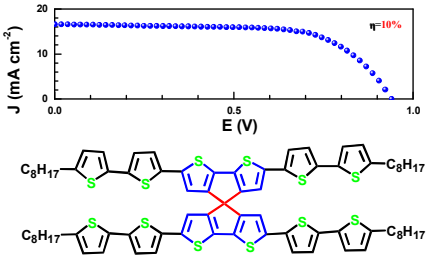

Journal of Materials Chemistry A Accepted Manuscript